CHEMISTRY OF
MATERIALS
Article

Chem. Mater. **2010,** *22,* 4069–4075
DOI:10.1021/cm100931r

Hierarchical Control of Polymer Composite Nano- and Micro-Structure with Lithography

Janine K. Nunes,[†] Merve Ertas,[†] Libin Du,[†] and Joseph M. DeSimone*,[†,‡]

[†]*Department of Chemistry, University of North Carolina at Chapel Hill, Chapel Hill, North Carolina 27599, and* [‡]*Department of Chemical and Biomolecular Engineering, North Carolina State University, Raleigh, North Carolina 27695*

Received April 2, 2010. Revised Manuscript Received May 20, 2010

We have developed a novel composite film fabrication process that utilizes the soft lithographic approach, Particle Replication in Nonwetting Templates (PRINT). This process was found to be a very viable approach to the fabrication of well-structured, multifunctional polymer composite thin films. Particle aggregation was completely eliminated as discretely molded particles with specific shape, size and composition were maintained in well-defined arrays determined by the silicon master template. Both all-organic and polymer-ceramic composites have been generated using this technique with particle inclusions ranging in size from 200 nm to 20 μm. The composition of the composite was well-controlled with both cross-linked and thermoplastic polymeric continuous phases, as well as particle compositions ranging from cross-linked polymeric resins to the inorganic oxide, barium titanate.

1. Introduction

The fabrication of multifunctional nanoengineered composite materials with enhanced properties has become increasingly important for a range of advanced technological applications[1] including actuators,[2] chemical/biological sensors,[3] flexible electronics,[4] and membranes.[5] To realize these structured materials, it is essential to be able to control the hierarchical nanostructure over multiple length scales for the precise manipulation of bulk properties. A primary concern in the field of polymer composites is the inability to effectively disperse nanoparticles, and thus avoid particle aggregation, which may inhibit many potential mechanical, optical or electrical benefits gained by adding the nanoparticles to the polymer matrix.[6,7] The surface functionalization of nanoparticles has long been a fundamental yet important strategy to prevent particle aggregation and agglomeration.[7−10] Additionally, different promising approaches have been developed to better control the composite nanostructure, including layer-by-layer (LbL) assembly,[11] block copolymer techniques,[12,13] self-assembly,[14] and the use of external fields.[15] Though quite effective on the nanoscale, many of these processes either cannot be directly scaled-up or are limited in the type of materials that can be used.

Lithographic processes have not been widely applied to the fabrication of ordered composites. The only type of lithography that has been used is interference lithography (IL).[16] IL has been successful at realizing uniform 3-D periodic polymeric structures. These porous architectures can be filled with a second component and polymerized to form bicontinuous composite films.[16] Additionally, periodic polymer/metal nanocomposites have been generated from the holographic patterning of photocurable monomers and metal precursors.[17,18] Imprint lithography, however, has not previously been used to directly control the nano- and microstructure of polymer/particle composites. Here we demonstrate a novel, scalable roll-to-roll fabrication process for well-structured polymer composite films with a high degree of nanostructure control and hierarchical

---

*To whom correspondence should be addressed. E-mail: desimone@unc.edu.

(1) Vaia, R. A.; Maguire, J. F. *Chem. Mater.* **2007**, *19*, 2736–2751.
(2) Vaia, R.; Baur, J. *Science* **2008**, *319*, 420–421.
(3) Lewis, N. S. *Acc. Chem. Res.* **2004**, *37*, 663–672.
(4) Katz, H. E.; Huang, J. *Annu. Rev. Mater. Res.* **2009**, *39*, 71–92.
(5) Mahajan, R.; Burns, R.; Schaeffer, M.; Koros, W. J. *J. Appl. Polym. Sci.* **2002**, *86*, 881–890.
(6) Balazs, A. C.; Emrick, T.; Russell, T. P. *Science* **2006**, *314*, 1107–1110.
(7) Krishnamoorti, R. *MRS Bull.* **2007**, *32*, 341–347.
(8) Dyke, C. A.; Tour, J. M. *J. Phys. Chem. A* **2004**, *108*, 11151–11159.
(9) Pyun, J.; Matyjaszewski, K. *Chem. Mater.* **2001**, *13*, 3436–3448.
(10) Usuki, A.; Kojima, Y.; Kawasumi, M.; Okada, A.; Fukushima, Y.; Kurauchi, T.; Kamigaito, O. *J. Mater. Res.* **1993**, *8*, 1179–1184.
(11) Podsiadlo, P.; Kaushik, A. K.; Arruda, E. M.; Waas, A. M.; Shim, B. S.; Xu, J.; Nandivada, H.; Pumplin, B. G.; Lahann, J.; Ramamoorthy, A.; Kotov, N. A. *Science* **2007**, *318*, 80–83.
(12) Sides, S. W.; Kim, B. J.; Kramer, E. J.; Fredrickson, G. H. *Phys. Rev. Lett.* **2006**, *96*, 250601–4.
(13) Zhao, Y.; Thorkelsson, K.; Mastroianni, A. J.; Schilling, T.; Luther, J. M.; Rancatore, B. J.; Matsunaga, K.; Jinnai, H.; Wu, Y.; Poulsen, D.; Frechet, J. M. J.; Alivisatos, A. P.; Xu, T. *Nat. Mater.* **2009**, *8*, 979–985.
(14) Krishnan, R. S.; Mackay, M. E.; Duxbury, P. M.; Pastor, A.; Hawker, C. J.; Van Horn, B.; Asokan, S.; Wong, M. S. *Nano Lett.* **2007**, *7*, 484–489.
(15) Koerner, H.; Hampton, E.; Dean, D.; Turgut, Z.; Drummy, L.; Mirau, P.; Vaia, R. *Chem. Mater.* **2005**, *17*, 1990–1996.
(16) Singamaneni, S.; Chang, S.; Jang, J.-H.; Davis, W.; Thomas, E. L.; Tsukruk, V. V. *Phys. Chem. Chem. Phys.* **2008**, *10*, 4093–4105.
(17) Sakamoto, M.; Fujistuka, M.; Majima, T. *J. Photochem. Photobiol., C* **2009**, *10*, 33–56.
(18) Vaia, R. A.; Dennis, C. L.; Natarajan, L. V.; Tondiglia, V. P.; Tomlin, D. W.; Bunning, T. J. *Adv. Mater.* **2001**, *13*, 1570–1574.

order. This fabrication process builds upon the Particle Replication in Nonwetting Templates (PRINT) technology, which offers exceptional control of composite nanostructure because the particle shape, size, orientation, composition, and modulus can be individually tuned.[19,20]

The PRINT process is a nanomolding technique where a low surface energy elastomeric mold is used to generate two-dimensional ordered arrays of monodisperse, shape-specific particles. The molds, derived from a photocurable liquid perfluoropolyether (PFPE) precursor, exhibit high gas permeability, exceptionally low surface energies (~10 dyn/cm), excellent solvent resistance, excellent release properties, and high thermal stability.[20] Furthermore, the molecular weight between cross-links can be systematically varied and as a result, the PFPE elastomers can accurately mold to within 1 nm resolution.[21] These properties render PFPE an ideal molding material for the production of arrays of discrete particles of a broad range of materials and as such, is an essential component in this approach to fabricating ordered polymer composite thin films. An important advantage of the PRINT process is that the particles are fabricated in an intrinsically non-aggregated state. Such a 2-dimensional array of nano- and microparticles thus enables simple strategies to be employed to transfer the particles to a matrix without aggregation to build up more complex, hierarchically ordered, 3-dimensional structures. Herein we describe the fabrication of polymer composites with complex 3-dimensional nano- and microarchitectures via the capture of 2-dimensional arrays of polymeric or ceramic particles in a polymeric continuous phase without aggregating the particles, followed by a layering and lamination step.

2. Experimental Section

Materials. The PFPE mold precursor (Fluorocur) was supplied by Liquidia Technologies. The monomers: PEG-DMA (M_n = 550 g/mol and 750 g/mol), trimethylolpropane ethoxylate triacrylate (M_n = 912 g/mol), and 1-vinyl-2 pyrrolidone were deinhibited with adsorption alumina prior to adding the photoinitiator (0.5 wt % DEAP). Poly[2-methoxy-5-(3′,7′-dimethyloctyloxy)-1,4-phenylenevinylene] (MDMO-PPV) (M_n = 23,000 g/mol) was solution processed as a 2 wt % solution in chlorobenzene. Polystyrene (M_n = 10,000 g/mol) was solution processed as a 35 wt % solution in tetrahydrofuran. The epoxy system used was a commercial 5-min 2-part epoxy adhesive (Fisher Scientific). Unless otherwise stated, all reagents were purchased from Sigma-Aldrich and used as received.

PRINT Particle Fabrication. The PFPE mold precursor (Fluorocur, Liquidia Technologies) was combined with 0.1 wt % 2,2-diethoxyacetophenone (DEAP) prior to spreading on the silicon master template, backing with a poly(ethylene terephthalate) (PET) sheet and photocuring. The molds were filled with particle monomer solutions using capillary filling and film splitting techniques described extensively elsewhere.[19,20,22,23]

Magnesium Oxide (MgO) Thin Film Preparation. A sol–gel method was used for the MgO thin film. The sol was prepared by dissolving 8.3 wt % magnesium nitrate hexahydrate and 16.7 wt % polyvinylpyrrolidone (Acros, M_n = 58,000 g/mol) in distilled water (75 wt %). Silicon wafers were cleaned in piranha solution (70% concentrated sulfuric acid and 30% hydrogen peroxide (30% in water)) prior to film deposition. The MgO sol was spin coated onto the wafer and heated to 485 °C for 5 min. This was repeated 4 times to build up a MgO film thickness of approximately 200 nm. The final film was annealed at 800 °C for 1 h.

$BaTiO_3$ Sol–Gel Synthesis and Particle Array Fabrication. The $BaTiO_3$ sol was prepared by first dissolving barium acetate in glacial acetic acid (42 wt %) at 80 °C. In a separate vessel, equimolar amounts of titanium^{IV} isopropoxide (equimolar to barium acetate) and acetylacetone were combined. The two solutions were mixed, and the sol was cooled to room temperature while stirring. The sol was diluted with 15 wt % 2-methoxyethanol, then filtered through a 0.45 μm syringe filter. This solution was used to fill the PFPE molds. The sol in the mold cavities was converted to the xerogel by heating to 85 °C, where the particles were able to retain the mold features. The xerogel particles were harvested with a thin layer of polycyanoacrylate adhesive (Zap CA PT-08, Pacer Technologies) onto a MgO-coated silicon wafer. MgO served as a sacrificial layer that was removed later in the fabrication process, and as it is lattice-matched with many ferroelectric and superconducting materials,[24] it was an appropriate substrate for the formation of these ceramic particles. After harvesting, the array was heated in air to 700 °C for 1 h to calcine and crystallize the ceramic particles then cooled at a rate of 10 °C/min. Bulk $BaTiO_3$ powder samples were characterized with an X-ray Diffractometer (XRD, Rigaku) using Cu Kα radiation.

Composite Film Fabrication. This PRINT composite film fabrication process was demonstrated for various polymer composite systems, which are summarized in Table 1. For the cross-linked matrix systems, a thin film of the continuous phase prepolymer, for example, a poly(ethylene glycol) dimethacrylate (PEG-DMA), was used as the adhesive to remove the particles from the mold. Additional continuous phase polymer was cast onto the array to cover the particles, and acted as the adhesive for a second layer of particles. This simple step was performed repeatedly to increase the composite thickness. For the thermoplastic matrix/cross-linked particles system, the particles were harvested directly onto a thin film of polycarbonate (PC; M_n = 45,000 g/mol). Multiple polymer/particle layers were stacked and melt pressed using a hydraulic press (PHI Manual Hydraulic Compression Press, 155 °C, 1100 psi). For the thermoplastic matrix/inorganic particles system, the $BaTiO_3$ particles were transferred to a thermoplastic continuous phase by casting a solution of the desired polymer onto the array. For poly(vinylidene fluoride) (PVDF; M_n = 107,000 g/mol) films, a 8 wt % PVDF in dimethylformamide (DMF, Fisher Scientific) solution was used and for PC films, a 6 wt % PC in chloroform (Fisher Scientific) solution was used. The single composite layer

---

(19) Gratton, S. E. A.; Williams, S. S.; Napier, M. E.; Pohlhaus, P. D.; Zhou, Z.; Wiles, K. B.; Maynor, B. W.; Shen, C.; Olafsen, T.; Samulski, E. T.; DeSimone, J. M. *Acc. Chem. Res.* **2008**, *41*, 1685–1695.

(20) Rolland, J. P.; Maynor, B. W.; Euliss, L. E.; Exner, A. E.; Denison, G. M.; DeSimone, J. M. *J. Am. Chem. Soc.* **2005**, *127*, 10096–10100.

(21) Maynor, B. W.; LaRue, I.; Hu, Z.; Rolland, J. P.; Pandya, A.; Fu, Q.; Liu, J.; Spontak, R. J.; Sheiko, S. S.; Samulski, R. J.; Samulski, E. T.; DeSimone, J. M. *Small* **2007**, *3*, 845–849.

(22) Hampton, M. J.; Williams, S. S.; Zhou, Z.; Nunes, J.; Ko, D.-H.; Templeton, J. L.; Samulski, E. T.; DeSimone, J. M. *Adv. Mater.* **2008**, *20*, 2667–2673.

(23) Merkel, T.; Herlihy, K.; Nunes, J.; Orgel, R.; DeSimone, J. M. *Langmuir* **2009**, DOI: 10.1021/la903890h.

(24) Fu, X.; Song, Z.; Wu, G.; Huang, J.; Duo, X.; Lin, C. *J. Sol-Gel Sci. Technol.* **1999**, *16*, 277–281.

Table 1. Summary of Fabricated PRINT Composite Systems

system	continuous polymer phase	discrete particle phase
cross-linked matrix/thermoplastic particles	cross-linked poly(ethylene glycol) (PEG)	polyvinylpyrrolidone
	cross-linked PEG	MDMO-PPV[a]
	cross-linked PEG	polystyrene
cross-linked matrix/cross-linked thermoset particles	cross-linked PEG	trimethylolpropane ethoxylate triacrylate resin
	cross-linked PEG	cross-linked PEG (different molecular weight between cross-links)
	epoxy resin	trimethylolpropane ethoxylate triacrylate resin
thermoplastic matrix/cross-linked thermoset particles	polycarbonate	cross-linked PEG
thermoplastic matrix/inorganic particles	polycarbonate	barium titanate ($BaTiO_3$)
	poly(vinylidene fluoride)	$BaTiO_3$

[a] MDMO-PPV: poly[2-methoxy-5-(3′,7′-dimethyloctyloxy)-1,4-phenylenevinylene].

can be gently pulled off the MgO/Si by hand, but for very thin films, it was more practical to dissolve the MgO layer with dilute hydrochloric acid to gently lift-off the composite layer to prevent damaging the film. The single layers can be stacked and melt-pressed (or laminated) to form the composite film using the hydraulic press at 1100 psi (155 °C for PC and 172 °C for PVDF). The films were held at those conditions for 10 min, and then allowed to cool below their glass transition temperatures while under pressure.

Instrumentation. Scanning Electron Microscope (SEM) images were taken on a Hitachi S-4700 SEM and environmental SEM micrographs were taken on a FEI Quanta 200 FEG instrument using a backscattered electron detector. Fluorescence images were taken on a Zeiss Axioskop 2MAT incident light microscope fitted with an AxiCam MRM digital camera. Confocal images were taken on a Zeiss LSM5 Pascal Confocal Laser Scanning Microscope. Dynamic Mechanical Analyzer (DMA) measurements were performed using a Perkin-Elmer Pyris Diamond DMA in tension mode at a frequency of 1 Hz. TGA measurements were performed on a Perkin-Elmer Pyris I Thermogravimetric Analyzer, heating from 25 °C−600 °C at a heating rate of 10 °C/min in a nitrogen atmosphere.

SEM Sample Preparation. To obtain cross-sectional images of the composite films, the films were immersed in liquid nitrogen and cut with a sharp blade. (Note that this treatment occasionally warped the films and broke the embedded ceramic particles.)

3. Results and Discussion

3.1. Cross-Linked Matrix Systems. In the simplest realization of the PRINT composite film fabrication process, the continuous phase polymer was used to harvest or remove the particles from the mold. The thickness of each layer, which was easily tuned by adjusting the spin coating parameters, dictated the vertical spacing between particles. Similarly, adjusting the layer thickness was one method used to control the particle volume fraction, where, for example, a minimum film thickness equal to the height of the particles in that layer would result in the maximum possible particle volume fraction for a given 2-D array and desired overall film thickness. Other film casting methods, such as the use of a Meyer rod, have also been successfully applied to control the layer thickness. This process was used to fabricate a variety of polymer/polymer composite films, and is described schematically in Figure 1a. Composite films were generated with thermoplastic particles, such as polyvinylpyrrolidone (PVP), polystyrene (PS), and the semiconducting polymer, MDMO-PPV. Thermoset particles, such as cross-linked trimethylolpropane ethoxylate triacrylate resin, were also incorporated into the composite. The composition of the continuous phase included both PEG-DMA and epoxy cross-linked systems. Typically, the final composite films were approximately 2 square inches large, though films were fabricated with dimensions as large as 6 in. (because the templates are patterned on 6 in. silicon wafers).

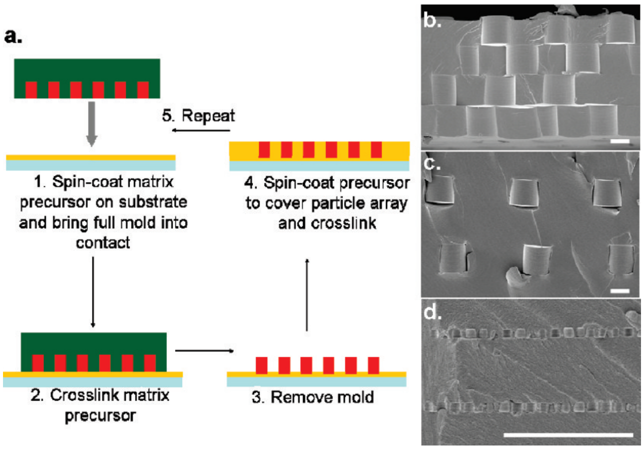

Figure 1. Ordered polymer/polymer composite films showing (a) simplified fabrication scheme and SEM images of cross sections of the resultant films where (b) is a PEG/triacrylate resin composite film with 7 μm cylindrical triacrylate particles, (c) is an epoxy/triacrylate resin composite film with 7 μm cylindrical triacrylate particles and (d) is a PEG/triacrylate resin composite film with 200 nm cylindrical triacrylate particles. Scale bars represent 4 μm.

The microstructure of the PRINT composite films was evident when the films were sectioned and imaged with SEM. In Figures 1b−d, the regular arrangement of uniform, cylindrical triacrylate resin particles is clearly identifiable in the continuous epoxy and PEG-DMA matrixes. Size control was demonstrated by varying the particle size from 7 μm to 200 nm. Particle packing within each layer was also controlled, as demonstrated by the square lattice arrangement of the 7 μm cylinders and the hexagonal packing of the 200 nm cylinders. The particle dimensions, horizontal particle spacing, and arrangement of the particles within each layer were precisely governed by the silicon master template used to fabricate the mold. This template,

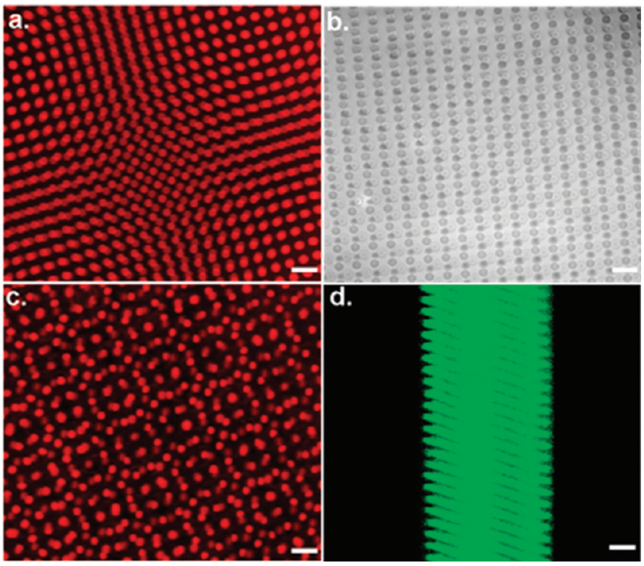

Figure 2. Optical images of ordered composite films where (a) is a top view fluorescence image of a PEG/triacrylate resin 2-layer composite film with 7 μm cylindrical triacrylate particles (rhodamine B dye used in particles for imaging), (b) is a top view DIC image of a PEG/PS 3-layer composite film with 7 μm cylindrical PS particles, (c) is a top-view fluorescence image of a PEG/MDMO-PPV 2-layer composite film with 7 μm cylindrical MDMO-PPV particles, and (d) is an angled view of the 3-D confocal microscopy projection of a PEG/PVP 3-layer composite film with 10 wt % Paclitaxel in the 5 μm cubic PVP inclusions (fluorescein *o*-acrylate dye used in particles for imaging). Scale bars represent 20 μm.

which was fabricated using standard photolithography, can be designed to have a preferred particle shape, size, spacing, and pattern with a high degree of spatial resolution. It is important to note that the particles in the composite films were not registered perpendicular to the plane of the film, as evidenced from the top-view fluorescence and DIC images of composite films with 7 μm cylindrical particles arranged on a square lattice within each layer (Figure 2a−c). Complex Moire patterns resulted from the pattern mismatch between layers, suggesting that these films may exhibit interesting optical properties.

The PEG-DMA/PVP ordered composite film was a particularly interesting example because the 1-vinyl-2-pyrrolidone monomer dissolves non-polar compounds such as the antiproliferative agent, Paclitaxel. A 3-D confocal microscopy projection of the PEG-DMA/PVP composite (containing 10 wt % Paclitaxel in the PVP particles) is presented in Figure 2d. PEG is a non-toxic, biocompatible polymer, and PVP is a common water-soluble excipient used in drug delivery applications. By varying the cross-link density of the PEG matrix in each layer, the release of the drug can potentially be controlled and sustained, thereby illustrating the potential for this fabrication to be used in generating thin films for local therapeutic treatment.

3.2. Thermoplastic Matrix Composites − Control of Particle Orientation.

Particle orientation is another property that can be controlled with this PRINT composite fabrication process. This was accomplished by rotating the individual layers. For example, two bilayer polycarbonate (PC) films containing highly anisotropic rectangular prism (20 × 4 × 5 μm) PEG-DMA cross-linked particles were fabricated: one with particle layers oriented parallel to each other and the other with particle layers oriented perpendicular to each other. To fabricate these composites, the free-standing PC/particle layers were stacked either with particles oriented in the same direction or one layer was rotated 90°, so that the particle layers were orthogonal. The layers were laminated at 155 °C, above the glass transition temperature of PC. Confocal microscopy was used to analyze the films (Figure 3). Figure 3a shows the film with parallel layers, as can be observed in the 3-D projection and the z-slices, the particle layers are pointing in the same direction (±5°). Conversely, in Figure 3b the particles in the two layers are clearly orthogonal. Additional evidence is shown in movies of rotating 3-D projections of the bilayers provided in the Supporting Information.

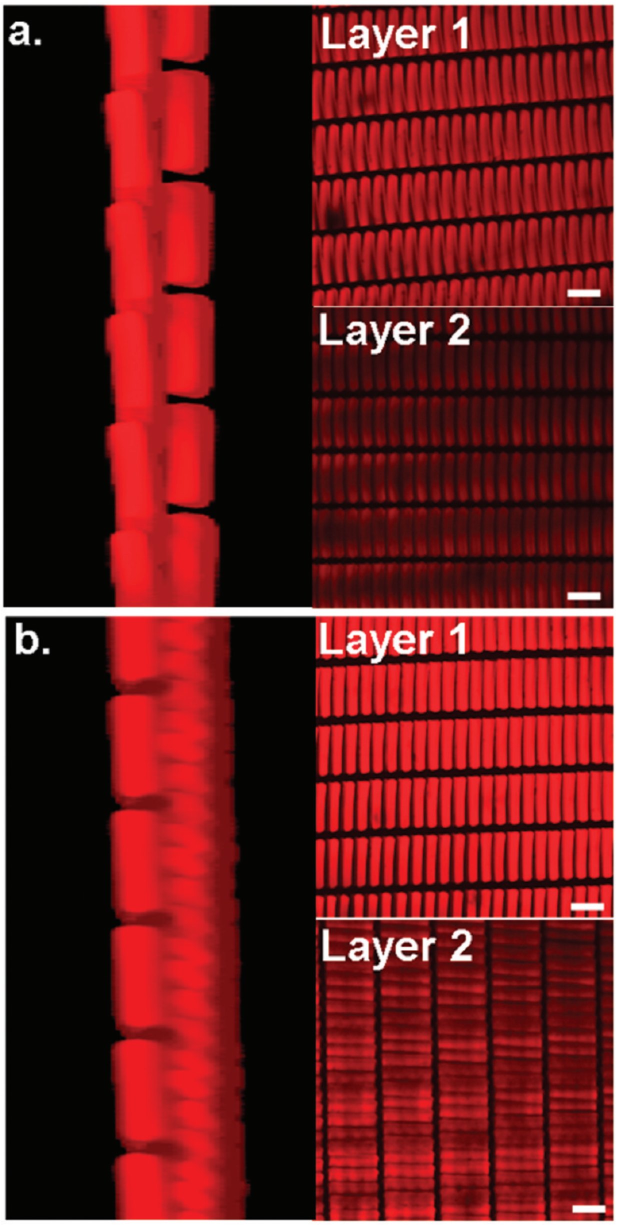

Figure 3. Confocal microscopy study of ordered PC/PEG bilayer composite films showing two different relative layer orientations where in (a) both particle layers are parallel and in (b) the particle layers are perpendicular. Scale bars represent 10 μm.

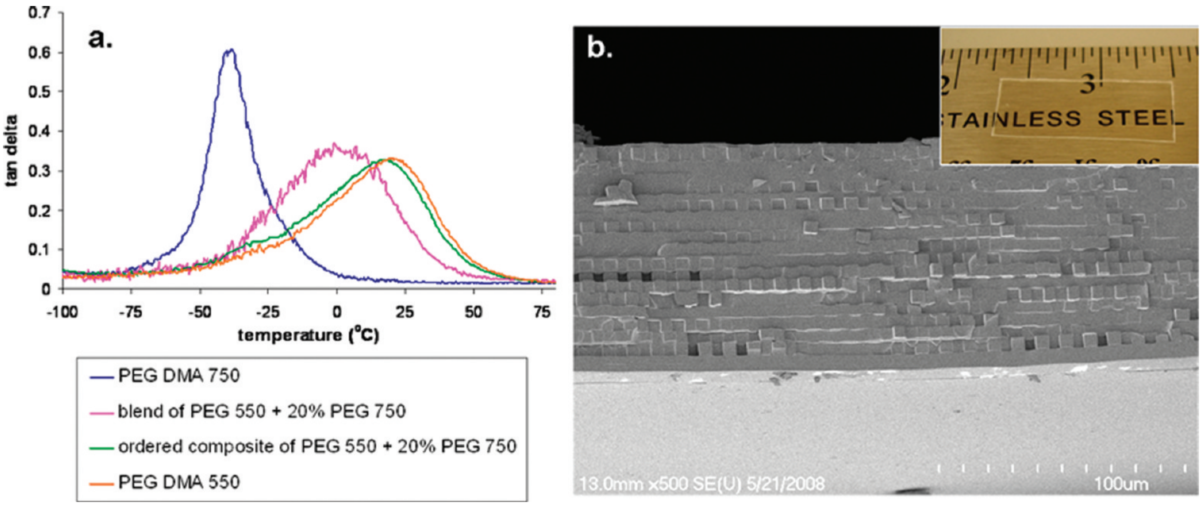

Figure 4. Dynamic Mechanical Analysis of an all-PEG composite where (a) shows the tan δ curves for pure 750 g/mol PEG-DMA, pure 550 g/mol PEG-DMA, a 4:1 solution of 750 g/mol PEG-DMA and 550 g/mol PEG-DMA and an ordered composite 4:1 750/550 g/mol PEG-DMA, and (b) is an SEM image of the ordered 4:1 750/550 g/mol PEG-DMA composite film cross-section containing 16 particle layers with an inset picture of the transparent film.

3.3. Phase-Separated Miscible Polymer Composites. Another remarkable advantage of this fabrication process is the ability to separate miscible polymeric systems into well-ordered phases. This can be valuable in fabricating materials with novel release profiles[25] or mechanical properties. For example, two PEG-DMA monomers of differing molecular weights were used to fabricate a cross-linked ordered composite film with the lower molecular weight monomer (M_n = 550 g/mol) as the continuous phase and the higher molecular weight monomer (M_n = 750 g/mol) as discrete 5 μm cubic particles. A transparent free-standing 16-layer PRINT composite thin film was fabricated, and the presence of the two cross-linked PEG phases with different cross-link densities was confirmed by Dynamic Mechanical Analysis (Figure 4). Glass transition temperatures (T_g), determined from tan δ peaks, were found to be −38.1 and 19.3 °C for pure cross-linked 750 g/mol PEG-DMA and 550 g/mol PEG-DMA, respectively. When the 550 g/mol PEG-DMA and 750 g/mol PEG-DMA monomers were blended to form a homogeneous solution (4:1 volume ratio) and then cross-linked, the gel was found to have a T_g of −0.8 °C. Conversely, the PRINT composite, with approximately the same prepolymer volume fraction as the homogeneous blend, had a tan δ peak at 18.2 °C, comparable to the T_g of 550 g/mol PEG-DMA (the continuous phase of the composite), with a slight shoulder at approximately −35 °C, which may be an indication of the 750 g/mol PEG-DMA cross-linked particle domains.

3.4. Hierarchially Ordered Polymer/Ceramic Composites. The use of the PRINT process to fabricate polymer composites can be extended to polymer/ceramic composites. These composite films are of high interest in the materials science field, as the piezoelectric material in electromechanical transducers, gate insulators in organic field-effect transistors, high energy density capacitors, and other electronic devices.[26−29] In particular, much research has been focused on the films of barium titanate ($BaTiO_3$) particles in polymer matrixes because of the high dielectric properties of $BaTiO_3$ for improved capacitor applications.[30] Various methods for fabricating polymer/$BaTiO_3$ composite films have been reported in the literature.[31−34] Recently, Kim and co-workers successfully demonstrated a technique to uniformly disperse high volume fractions of $BaTiO_3$ nanoparticles throughout different polymer matrixes.[27,32] Their technique involved the surface functionalization of commercially available $BaTiO_3$ nanoparticles with tailored organic phosphonic acid ligands before incorporation into the polymer systems. The dielectric properties of these composite films strongly depended on the size/shape of the crystallites and the domain configuration of the $BaTiO_3$ nanoparticles, as well as the volume fraction of the particles.[35] Here, we demonstrate the fabrication of polymer/$BaTiO_3$ composite films using PRINT technology. Unlike the other techniques in the literature, the PRINT process can easily control the shape, size, and also the volume fraction of $BaTiO_3$ particles in the polymer matrix.

For the ordered polymer/ceramic composites, it was necessary to modify some of the steps described previously

---

(25) Lu, S.; Anseth, K. S. *J. Controlled Release* **1999**, *57*, 291–300.
(26) Feenstra, J.; Sodano, H. A. *J. Appl. Phys.* **2008**, *103*, 124108-5.
(27) Kim, P.; Doss, N. M.; Tillotson, J. P.; Hotchkiss, P. J.; Pan, M.-J.; Marder, S. R.; Li, J.; Calame, J. P.; Perry, J. W. *ACS Nano* **2009**, *3*, 2581–2592.
(28) Lott, J.; Xia, C.; Kosnosky, L.; Weder, C.; Shan, J. *Adv. Mater.* **2008**, *20*, 3649–3653.
(29) Schroeder, R.; Majewski, L. A.; Grell, M. *Adv. Mater.* **2005**, *17*, 1535–1539.
(30) Kobayashi, Y.; Kurosawa, A.; Nagao, D.; Konno, M. *Polym. Eng. Sci.* **2009**, *49*, 1069–1075.
(31) Guo, N.; DiBenedetto, S. A.; Kwon, D.-K.; Wang, L.; Russell, M. T.; Lanagan, M. T.; Facchetti, A.; Marks, T. J. *J. Am. Chem. Soc.* **2007**, *129*, 766–767.
(32) Kim, P.; Jones, S. C.; Hotchkiss, P. J.; Haddock, J. N.; Kippelen, B.; Marder, S. R.; Perry, J. W. *Adv. Mater.* **2007**, *19*, 1001–1005.
(33) Ramesh, S.; Shutzberg, B. A.; Huang, C.; Jie, G.; Giannelis, E. P. *Adv. Packag., IEEE Trans.* **2003**, *26*, 17–24.
(34) Tomer, V.; Randall, C. A.; Polizos, G.; Kostelnick, J.; Manias, E. *J. Appl. Phys.* **2008**, *103*, 034115−7.
(35) Calame, J. P. *J. Appl. Phys.* **2006**, *99*, 084101−11.

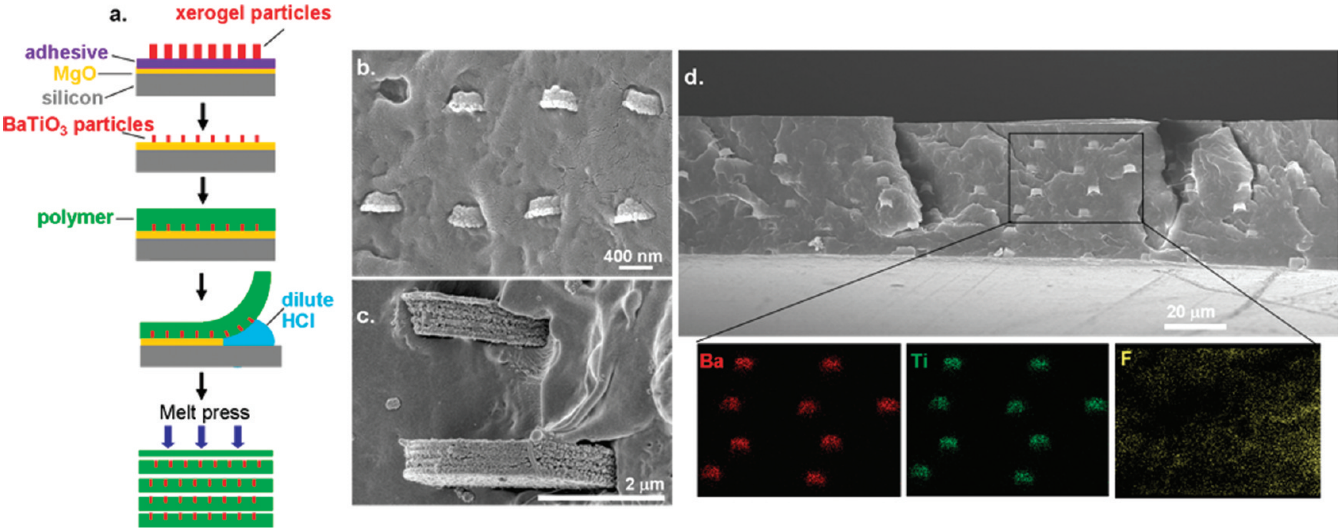

Figure 5. Ordered polymer/ceramic composite films showing (a) simple fabrication scheme with SEM images of examples of PVDF/$BaTiO_3$ film cross sections with (b) 400 × 200 nm cylinders, (c) 3 × 0.52 μm cylindrical particles, and (d) 3 × 2 μm cylindrical particles, with Energy Dispersive Spectroscopy elemental mapping identifying the Ba and Ti from the ceramic particles and the F from the polymer.

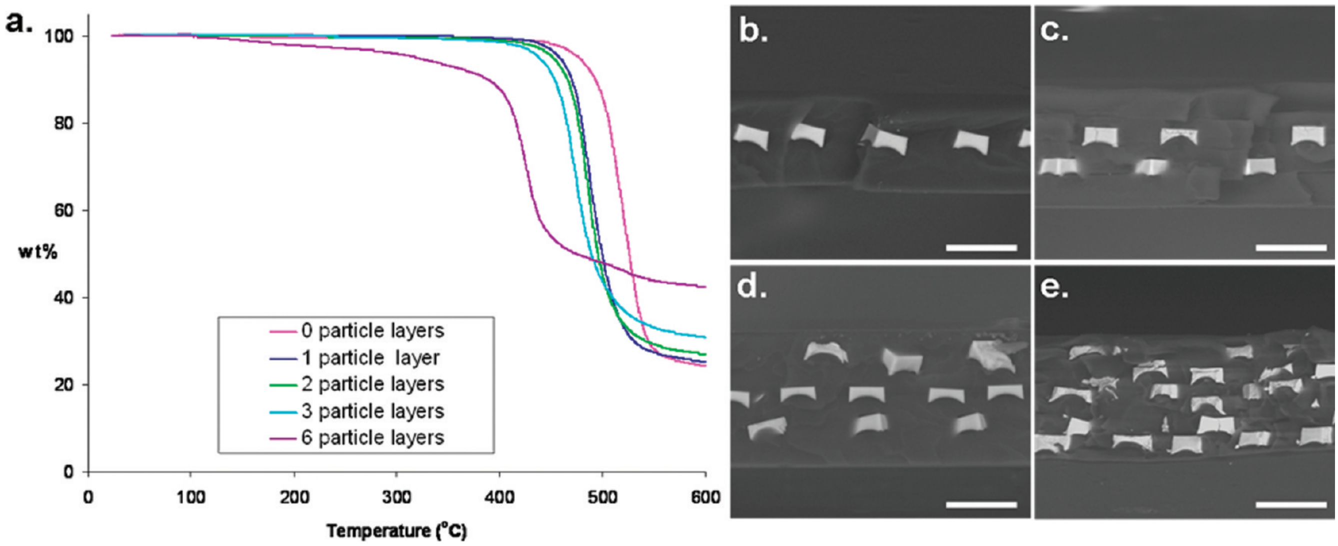

Figure 6. TGA study of PC/$BaTiO_3$ ordered composite films where (a) shows the decomposition curves for films with increasing number of particle layers and ESEM images of the composite film cross sections with (b) 1, (c) 2, (d) 3, and (e) 6 particle layers. Scale bars represent 10 μm.

for the polymer/polymer composites as the ceramic particles cannot be calcined while in the mold. This is because sol–gel-derived ceramic particles are typically calcined at temperatures far exceeding the decomposition temperature of the PFPE elastomer.[22] The model inorganic oxide, $BaTiO_3$, was used to demonstrate the composite fabrication in this work, though we have previously reported on the ability to fabricate particle arrays of numerous inorganic oxides.[22] An important characteristic of the calcination step was a 50% reduction in both the height and the width of the particles. Thus, templates were used that had feature dimensions double the desired size. This process is illustrated schematically in Figure 5a. Cross-linked matrixes were used as well with the ceramic particles by casting the monomer onto the array, partially photocuring, and then lifting off. A second layer was added by placing the first partially cured composite layer onto a second array with uncured monomer—the two layers were completely cured and then lifted off. Subsequent layers were added similarly.

Free-standing PVDF/$BaTiO_3$ composite film examples are shown in Figures 5b–d, with 400 × 200 nm, 3 × 0.52 μm, and 3 × 2.5 μm cylindrical particles. Similar to the polymer/polymer composite films, the polymer/ceramic composites exhibited exceptionally well-controlled, non-aggregated nano- and microstructure. Starting at the smallest length scale were the nanosized crystalline domains (10–50 nm) of the $BaTiO_3$ particles (cubic crystalline phase, as determined by X-ray diffraction), then extending out was another length scale defining the shape of the polycrystalline ceramic particle (nm to μm), followed by the length scales characterizing the spacing between particles both laterally and vertically (nm to μm), then finally the macroscopic dimensions of the composite film (μm to cm). Thus, these ordered composite films can be controlled and characterized at all levels of structural hierarchy.

With the control that the PRINT process affords in composite film fabrication, it is possible to investigate structure−property relationships. A very simple manifestation of this was to vary the $BaTiO_3$ weight fraction in $PC/BaTiO_3$ ordered composite films, while maintaining uniform shape, size, spacing, and orientation of the particles, as well as thickness of the composite films, and then monitor the changes in thermal degradation properties of the composite with Thermogravimetric Analysis (TGA). $PC/BaTiO_3$ films were prepared with $5 \times 5 \times 2$ μm particle inclusions, and the particle shape was a rectangular prism with one concave side (resulting from meniscus formation during mold filling). A series of films were fabricated with the $BaTiO_3$ content varying from 0 wt % to 18.4 wt %. The TGA curves exhibited a clear trend in decreasing thermal stability with increasing $BaTiO_3$ content (Figure 6). The decomposition temperature (at 5% weight loss) decreased linearly with increasing $BaTiO_3$ wt % except at the highest weight fraction measured. These $BaTiO_3$ ordered composite films are the focus of ongoing studies as they are very relevant to the field of capacitor dielectrics, where the major engineering challenge is to avoid particle aggregation.[35,36]

4. Conclusions

We have described a versatile, scalable composite film fabrication process that allows for the tailoring of composite film nano- and microstructures. Films were fabricated with different material combinations to yield structurally complex films with well-defined morphologies in which uniformly shaped polymeric or inorganic particles of one component were evenly dispersed with a desired periodicity within the other component. As the PRINT process is a versatile and general platform technology that is compatible with a broad range of particle compositions, from sensitive, biologically active materials requiring extremely mild conditions[37] to the relatively harsh chemistries of ceramics,[22] a wide range of materials can be incorporated into the ordered composites. Moreover, the scalability of the PRINT process has been demonstrated commercially with continuous manufacturing,[23,38] and so the techniques described herein can be readily adapted to roll-to-roll technology. For the case of polymer/polymer composite films, to attain the same morphological control via the blending of immiscible polymers, stringent control of numerous processing conditions is required.[39] Additionally, the PRINT polymer composite films have domain sizes and morphologies that rival blended polymer and block copolymer systems; and unlike these other approaches, with the PRINT process it is possible to take polymers that are typically miscible, and produce composites with well-ordered domains.

Acknowledgment. The authors acknowledge Dr. Douglas E. Betts for useful discussions; Dr. C. Robert Bagnell Jr. for assistance with confocal microscopy; David G. Vellenga and Chris Hardiman at the North Carolina State University Nanofabrication Facility for assistance with silicon master template fabrication; and Liquidia Technologies for the Fluorocur. This work was supported in part by the Schlumberger Faculty for the Future Fellowship, the STC program of the National Science Foundation (Agreement no. CHE-9876674), the Office of Naval Research (N00014-08-1-0978), and the Chancellor's Eminent Professorship at the University of North Carolina at Chapel Hill. Conflict of Interest Disclosure: J.M.D. is co-founder of Liquidia Technologies that has licensed the technology reported in this paper.

Supporting Information Available: Movies of rotating 3-D projections of bilayer ordered composite films. This material is available free of charge via the Internet at http://pubs.acs.org.

---

(36) Brosseau, C.; Beroual, A.; Boudida, A. *J. Appl. Phys.* **2000**, *88*, 7278–7288.

(37) Kelly, J. Y.; DeSimone, J. M. *J. Am. Chem. Soc.* **2008**, *130*, 5438–5439.

(38) Canelas, D. A.; Herlihy, K. P.; DeSimone, J. M. *Wiley Interdiscip. Rev.: Nanomed. Nanobiotechnol.* **2009**, *1*, 391–404.

(39) Tran-Cong-Miyata, Q.; Nishigami, S.; Ito, T.; Komatsu, S.; Norisuye, T. *Nat. Mater.* **2004**, *3*, 448–451.